

The selective COX-2 inhibitor celecoxib modulates sphingolipid synthesis^S

Susanne Schiffmann,¹ Jessica Sandner, Ronald Schmidt, Kerstin Birod, Ivonne Wobst, Helmut Schmidt, Carlo Angioni, Gerd Geisslinger, and Sabine Grösch

Institut für Klinische Pharmakologie, Klinikum der Johann Wolfgang Goethe-Universität, Theodor-Stern-Kai 7, 60590 Frankfurt/Main, Germany

Abstract Sphingolipids such as ceramides (Cers) play important roles in cell proliferation, apoptosis, and cell cycle regulation. An increased Cer level is linked to the cytotoxic effects of several chemotherapeutics. Various selective cyclooxygenase-2 (COX-2) inhibitors induce anti-proliferative effects in tumor cells. We addressed the possible interaction of the selective COX-2 inhibitors, coxibs, with the sphingolipid pathway as an explanation of their anti-proliferative effects. Sphingolipids were measured using liquid chromatography tandem mass spectrometry. Treatment of various cancer cell lines with celecoxib significantly increased sphinganine, C_{16:0}, C_{24:0}, C_{24:1}-dihydroceramide (dhCer) and led to a depletion of C_{24:0}, C_{24:1}-Cer in a time- and concentration-dependent manner, whereas other coxibs had no effect. Using ¹³C, ¹⁵N-labeled L-serine, we demonstrated that the augmented dhCers after celecoxib treatment originate from de novo synthesis. Celecoxib inhibited the dihydroceramide desaturase (DEGS) in vivo with an IC₅₀ of 78.9 ± 1.5 μM and increased total Cer level about 2-fold, indicating an activation of sphingolipid biosynthesis. Interestingly, inhibition of the sphingolipid biosynthesis by specific inhibitors of L-serine palmitoyltransferase diminished the anti-proliferative potency of celecoxib. **In conclusion**, induction of de novo synthesis of sphingolipids and inhibition of DEGS contribute to the anti-proliferative effects of celecoxib.—Schiffmann, S., J. Sandner, R. Schmidt, K. Birod, I. Wobst, H. Schmidt, C. Angioni, G. Geisslinger, and S. Grösch. **The selective COX-2 inhibitor celecoxib modulates sphingolipid synthesis.** *J. Lipid Res.* 2009. 50: 32–40.

Supplementary key words cancer • cyclooxygenase-2 • apoptosis • dihydroceramide desaturase • ceramide • dihydroceramide

Sphingolipids constitute an essential component of the eucaryotic plasma membrane and are also utilized as an important second messenger in a variety of cellular events, including cell senescence, cellular differentiation, apoptosis, and proliferation (1–3). Endogenous sphingolipid lev-

els can be controlled by activation of sphingomyelinases (SMases) and de novo synthesis as well as by specific degradation mechanisms (e.g., ceramidases, lyases). The sphingolipid biosynthesis commences in the endoplasmic reticulum with the condensation of palmitoyl-CoA and L-serine by L-serine palmitoyltransferase (L-SPT). The intermediate 3-ketosphinganine is rapidly converted into sphinganine (dhSph) by 3-ketosphinganine reductase. Acyl-CoA thioesters of variable chain lengths are then attached to dhSph by chain-length-specific (dihydro)ceramide synthases (CerSs) (4). Dihydroceramide desaturase (DEGS) introduces a 4, 5-*trans* double bond in dihydroceramides (dhCers), resulting in formation of the final product, Cer. Via sphingosine (Sph), Cer is metabolized by the enzymes ceramidase and sphingosine kinase to sphingosine-1-phosphate (Sph1P). In the Golgi apparatus, the polar group phosphatidylcholine is attached to Cer by sphingomyelinase to produce sphingomyelin. SMase catalyzes the reverse reaction. Glucosylceramide synthase (GCS) transfers activated glucose to Cer to form glucosylceramide, which is the principle component of most glycosphingolipids (Fig. 1).

Cer, Sph, and dhSph all have been shown to activate a number of enzymes involved in stress signaling cascades, including both protein kinases and protein phosphatases that suppress growth and survival pathways upstream of apoptotic events (2, 5, 6). By contrast, Sph1P can potently induce cell proliferation through binding to Sph1P receptors, of which five are known (7, 8).

Coxibs have been shown to induce apoptosis and cell cycle arrest in various types of cancer cells, including colon,

Abbreviations: Cer, ceramide; CerS, (dihydro)ceramide synthase; C8-CPPC, C8-cyclopropenylceramide; COX-2, cyclooxygenase-2; DEGS, dihydroceramide desaturase; dhCer, dihydroceramide; dhSph, sphinganine; dhSph1P, sphinganine-1-phosphate; FB1, fumonisin B1; FCS, fetal calf serum; GCS, glucosylceramide synthase; HPLC, high-performance liquid chromatography; LC-MS/MS, liquid chromatography tandem mass spectrometry; SMase, sphingomyelinase; Sph, sphingosine; Sph1P, sphingosine-1-phosphate; Sph1PP, sphingosine-1-phosphate phosphatase; L-SPT, L-serine palmitoyltransferase.

¹To whom correspondence should be addressed.

e-mail: susanne.schiffmann@med.uni-frankfurt.de

^SThe online version of this article (available at <http://www.jlr.org>) contains supplementary data in the form of five figures.

This work was supported by the Deutsche Forschungsgemeinschaft Forschergruppe FOG 784/TP5 (GR2011/2-1).

Manuscript received 6 March 2008 and in revised form 3 July 2008 and in revised form 4 August 2008.

Published, JLR Papers in Press, 18 August 2008.
DOI 10.1194/jlr.M800122-JLR200

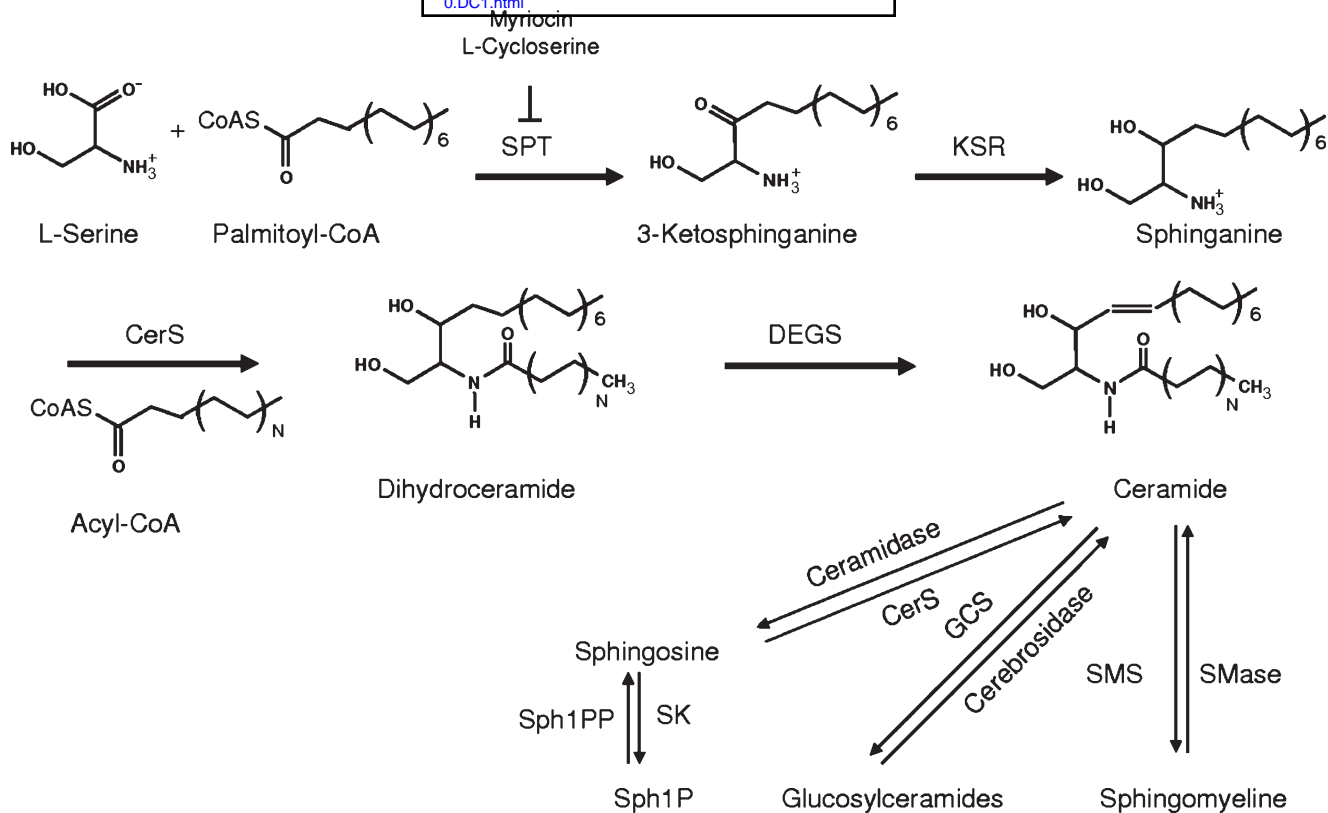


Fig. 1. Scheme of the sphingolipid pathway. L-SPT, L-serine palmitoyltransferase; KSR, 3-ketosphinganine reductase, CerS, (dihydro)ceramide synthase, DEGS, dihydroceramide desaturase, SMS, sphingomyeline synthase, SMase, sphingomyelinase, GCS, glucosylceramide synthase, SK, sphingosine kinase, Sph1PP, sphingosine 1-phosphate phosphatase, Sph1P, sphingosine 1-phosphate.

breast, lung, and cervical cancers (9–12). In addition to inhibition of cyclooxygenase-2 (COX-2), which is a key enzyme in the conversion of arachidonic acid to prostaglandins, COX-2-independent mechanisms are known to contribute to the anti-proliferative effects of coxibs (13). Treatment of clinical trial patients with celecoxib or rofecoxib produced pronounced reduction of the occurrence of colorectal adenomas relative to placebo (14–17).

The molecular mechanisms through which celecoxib or other coxibs exert their cytotoxic effects are not completely understood. Interestingly, celecoxib influences the β -catenin (5, 18) and caspase signaling pathways (19–21), which are also targets of sphingolipids. Celecoxib, therefore, may mediate its cytotoxic effects via modulation of sphingolipid metabolism. In addition, altered sphingolipid levels mediate the cytotoxic effects of several chemotherapeutics, such as etoposide (22, 23), paclitaxel (24), and *N*-(4-hydroxyphenyl) retinamide (25). Therefore, we hypothesize that the sphingolipid pathway may be an important target for the anti-proliferative effects of coxibs.

MATERIALS AND METHODS

Cells and reagents

The human cancer cell lines HCA-7, MCF-7, MDA-MB231, and HT-29 were purchased from European Collection of Cell Cultures (ECC; Salisbury, UK), and HEK293 and HCT-116 carcinoma cells were ordered from Deutsche Sammlung für

Mikroorganismen und Zellkulturen (DSMZ; Braunschweig, Germany). HEK293, MCF-7, and MDA-MB231 cells were cultured in DMEM without sodium pyruvate, containing glucose (4,500 mg/l) and GlutaMAX™. HCA-7 cells were cultured in DMEM containing sodium pyruvate, pyridoxine, and 8 mM L-glutamine. HCT-116 cells were incubated in McCoy's 5A medium, and HT-29 cells were cultured in RPMI medium containing GlutaMAX™ and 50 mM HEPES. All media contained 100 U/ml penicillin G and 100 μ g/ml streptomycin, 10% fetal calf serum (FCS) for culturing, and 7.5% FCS for treatment. Cells were cultured at 37°C in an atmosphere containing 5% CO₂. ¹³C₃, ¹⁵N-labeled L-serine, myriocin, desipramine, L-cycloserine, glutathione, par-nitrophenylphosphate, alkaline phosphatase, cholesterol, palmitic acid, and 1-phenyl-2-palmitoylamino-3-morpholino-1-propanol were purchased from Sigma-Aldrich (Schnelldorf, Germany). Fumonisin B1 (FB1) was purchased from Alexis Biochemicals (Lausen, Switzerland). C8-cyclopropenylceramide (C8-CPPC) was purchased from Matreya LLC (Pleasant Gap, PA). The sphingolipids were purchased either from Avanti Polar Lipids (Alabaster, AL) or Matreya LLC. Celecoxib, valdecoxib, etoricoxib, methylcelecoxib, and rofecoxib were synthesized by WITEGA Laboratorien Berlin-Adlershof GmbH. Lumiracoxib was provided by Novartis (Basel, Switzerland). The identity and purity of all coxibs were determined using [¹H]NMR spectroscopy and HPLC as described previously (26) and were >99%.

Determination of sphingolipid amounts in cells

For the quantification of sphingolipid amounts, cells were seeded at a density of 0.5×10^6 and incubated for 24 h. Cells subsequently were treated with various coxib concentrations (0–200 μ M) over various periods of time. The cells were washed with 1 ml PBS, treated with 0.5 ml trypsin, and collected in 0.5 ml PBS.

Cells were counted in a Neubauer chamber and centrifuged at 745 *g* and 4°C for 5 min. The PBS supernatant was removed, and the cells were stored at -80°C. Lipids were extracted with 200 μ l methanol after the addition of the internal standards (C_{17:0}-Cer, C_{17:0}-Sph, C_{17:0}-Sph1P). The suspension was incubated at 25°C with shaking at 1,400 rpm for 30 min and then centrifuged for 30 min at 25°C and 20,500 *g*. The supernatants were collected, and the extraction step was repeated. The combined organic phases were dried under a stream of nitrogen and resolved in methanol for quantification. After liquid-liquid extraction, amounts of C_{16:0}-Cer, C_{24:1}-Cer, C_{24:0}-Cer, C_{16:0}-dhCer, C_{24:1}-dhCer, C_{24:0}-dhCer, dhSph, Sph, sphinganine-1-phosphate (dhSph1P), and Sph1P, labeled analogs and the internal standards were determined by liquid chromatography coupled to tandem mass spectrometry (LC-MS/MS). Chromatographic separation was accomplished under gradient conditions using a Luna C18 column (150 mm \times 2 mm ID, 5 μ m particle size, and 10 nm pore size; Phenomenex, Aschaffenburg, Germany). The HPLC mobile phases consisted of water-formic acid (100:0.1, v/v) (A) and acetonitrile-tetrahydrofuran-formic acid (50:50:0.1, v/v/v) (B). A gradient program was used for the HPLC separation at a flow rate of 0.3 ml/min. The initial buffer composition 60% (A) / 40% (B) was hold for 0.6 min, then linearly changed to 0% (A) / 100% (B) in 4.4 min and hold for 5 min, then linearly changed to 60% (A) / 40% (B) in 0.5 min and hold for further 5.5 min. Ten microliters of each sample was injected, and the total run time was 16 min. MS/MS analyses were performed on an API 4000 triple quadrupole mass spectrometer with a Turbo V source (Applied Biosystems; Darmstadt, Germany). Precursor-to-product ion transitions of *m/z* 408 \rightarrow 264 for C_{8:0}-Cer, of *m/z* 538 (541) \rightarrow 264 (267) for C_{16:0}-Cer (C_{16:0}-Cer*), of *m/z* 648 (651) \rightarrow 264 (267) for C_{24:1}-Cer (C_{24:1}-Cer*), of *m/z* 651 (654) \rightarrow 264 (267) for C_{24:0}-Cer (C_{24:0}-Cer*), of *m/z* 540 (543) \rightarrow 284 (287) for C_{16:0}-dhCer (C_{16:0}-dhCer*), of *m/z* 651 (654) \rightarrow 284 (287) for C_{24:1}-dhCer (C_{24:1}-dhCer*), of *m/z* 653 (657) \rightarrow 284 (287) for C_{24:0}-dhCer (C_{24:0}-dhCer*), of *m/z* 300 (303) \rightarrow 282 (285) for Sph (Sph*), of *m/z* 302 (305) \rightarrow 284 (287) for dhSph (dhSph*), of *m/z* 380 (383) \rightarrow 264 (267) for Sph1P (Sph1P*), of *m/z* 382 (385) \rightarrow 266 (269) for dhSph1P (dhSph1P*), of *m/z* 300 (303) \rightarrow 270 (273) for 3-ketosphinganine (3-ketosphinganine*), of *m/z* 552 \rightarrow 534 for C_{17:0}-Cer, of *m/z* 286 \rightarrow 268 for C_{17:0}-Sph and of *m/z* 366 \rightarrow 250 for C_{17:0}-Sph1P were used for multiple reaction monitoring with a dwell time of 15 msec. Concentrations of the calibration standards, quality controls, and unknowns were evaluated by Analyst software 1.4.2 (Applied Biosystems). A representative chromatogram of C_{16:0}-Cer, C_{24:1}-Cer, C_{24:0}-Cer, C_{16:0}-dhCer, C_{24:1}-dhCer, C_{24:0}-dhCer, and dhSph is displayed in Supplementary Figure I. Suppression effects were assessed by extraction of cell samples (*n* = 6), which were reconstructed with 10 ng/ml internal standard in methanol. The mean peak areas of the samples reconstructed with internal standard were compared with the mean peak area of the internal standard in methanol. An ion suppression effect was observed between 15% and 25% for the internal standard. Linearity of the calibration curve was proven for 3-ketosphinganine, C_{24:0}-Cer, C_{24:1}-Cer from 1.5 to 300 ng/ml, for C_{16:0}-Cer, C_{16:0}-dhCer, C_{24:0}-dhCer, C_{24:1}-dhCer from 2 to 1,000 ng/ml, dhSph, Sph, Sph1P from 0.4 to 400 ng/ml. The coefficient of correlation for all measured sequences was at least 0.99. Variations in accuracy and intraday and interday precision [*n* = 2 for each concentration in five various cell lines (HCT-116, HeLa, HCA-7, MCF-7, and HEK293)] were less than 15% over the range of calibration.

In vitro cell viability assay

The WST-1 assay (Roche Diagnostic GmbH; Mannheim, Germany) was used to determine the viability and proliferation rate of the cells after treatment with coxibs and the various inhibitors

of sphingolipid biosynthesis. The cells were seeded at a density of 2–5 \times 10⁴ cells/well in 100 μ l of culture medium in 96-well microplates and incubated for 24 h at 37°C under an atmosphere containing 5% CO₂. Medium was removed, and the cells were treated with increasing concentrations of celecoxib for 20 h in the presence or the absence of myriocin (150 nM) and L-cycloserine (500 μ M) (inhibitors of L-SPT). The inhibitors were preincubated for 90 min. After 20 h of incubation, 10 μ l of WST-1 reagent was added to each well, and the cells were incubated for 90 min. The absorbance of the dye was measured at 450 nm against a reference wavelength of 620 nm using a 96-well spectrophotometric plate reader (SPECTRAFluor Plus, Tecan; Crailsheim, Germany).

Apoptosis assay

Induction of apoptosis after celecoxib treatment was measured by the APOPercentage apoptosis assay (Biocolor; Dublin, Ireland). This assay is dye-based and takes advantage of the phosphatidylserine transmembrane movement that takes place during the onset of apoptosis. When this occurs, the dye is able to penetrate the cell membrane and accumulates inside the cell. HCT-116 cells/well (15 \times 10⁴) were seeded in 100 μ l of 0.4% gelatin and 200 μ l of medium in 96-well plates. HCT-116 cells were either treated with 80 μ M celecoxib or coinubated with 80 μ M celecoxib and 150 nM myriocin for 6 h. The dye was added 30 min before analysis. For quantification of apoptosis, analytical digital photomicroscopy was used according to the manufacturer's manual.

Activity assay for L-SPT and CerS

For the L-SPT and CerS assay, the microsomal fraction of HCT-116 cells was isolated. The reaction mixture for the L-SPT assay contained 100 μ g of the microsomal fraction, 1 mM L-serine, 150 μ M palmitoyl-CoA, 50 μ M pyridoxal phosphate, 100 mM HEPES, 2.5 mM EDTA, and 5 mM DTT (pH 7.4). The assay mixture was preincubated for 10 min at 37°C. The reaction was initiated by the simultaneous addition of pyridoxal phosphate and palmitoyl-CoA, and the mixture was incubated for different time points (5, 10, 15, 20 min). For the CerS assay, the reaction mixture consisted of 50 μ g of the microsomal fraction, 30 μ M dhSph, 40 μ M palmitoyl-CoA in 20 mM HEPES, and 2 mM MgCl₂ (pH 7.4). After 10 min of preincubation at 37°C, the reaction was initiated by the addition of palmitoyl-CoA, and the mixture was incubated for different time points (5, 10, 15, 30 min). Both reactions were terminated by the addition of the extraction solvent chloroform-methanol (7:1). The extraction step was repeated, and the organic solution was separated and dried under a stream of nitrogen. The products, 3-ketosphinganine (L-SPT assay) and C_{16:0}-dhCer (CerS assay) were measured using LC-MS/MS. The specific activity was calculated based on the values of different time points.

Statistics

Proliferation and sphingolipid data are presented as mean \pm SEM. The IC₅₀ value was calculated using a nonlinear regression analysis and a sigmoidal E_{max} model. SPSS 9.01 software was used for statistical analyses. The sphingolipid levels and the cell viability rates were analyzed using an independent *t*-test, and the confidence interval was set at 95%.

RESULTS

Concentration-dependent alteration of the sphingolipid levels in HCT-116 cells after treatment with coxibs

We first investigated whether coxibs have an influence on the sphingolipid pathway in the human colon carcinoma

cell line HCT-116 after a 2 h treatment with various coxibs (rofecoxib, etoricoxib, valdecoxib, lumiracoxib, methylcelecoxib, and celecoxib). Subsequently, the cells were harvested and the sphingolipids isolated and determined by LC-MS/MS (27). As shown in **Fig. 2A**, celecoxib, and its close structural derivative methylcelecoxib, significantly increased $C_{16:0}$, $C_{24:1}$ and $C_{24:0}$ -dhCers and dhSph. Under the same conditions, celecoxib and methylcelecoxib decreased $C_{24:1}$ and $C_{24:0}$ -ceramides. In contrast, the levels of $C_{14:0}$, $C_{16:0}$, $C_{18:1}$, $C_{18:0}$, and $C_{20:0}$ -ceramides, sphingosine, Sph1P, and dhSph1P were not influenced by coxib treatment (data only shown for celecoxib, Supplement 2). Because of this result, we focused our efforts on the sphingolipids ($C_{16:0}$, $C_{24:1}$, $C_{24:0}$ -dhCer, $C_{24:1}$, $C_{24:0}$ -ceramide, and dhSph) that are affected by celecoxib and methylcelecoxib. Other COX-2 inhibitors, such as etoricoxib (up to 200 μ M), valdecoxib (up to 200 μ M), rofecoxib (up to

100 μ M), and lumiracoxib (up to 200 μ M), showed no influence on any of the tested sphingolipids even at very high concentrations, indicating that the effect of celecoxib and methylcelecoxib is substance specific and occurs independently of COX-2 inhibition. Celecoxib-modulated changes in sphingolipid levels were concentration dependent and detectable after a 2 h treatment of HCT-116 cells with 20 μ M celecoxib (**Fig. 2B**). The effect is more pronounced, however, with 80 μ M celecoxib, the concentration used in further experiments.

Celecoxib influences the sphingolipid levels in several cancer cell lines

To demonstrate that the effects of celecoxib on the sphingolipid levels are not cell type-specific, we measured sphingolipid levels in different human cancer cell lines after treatment with 80 μ M celecoxib for 2 h. **Figure 3**

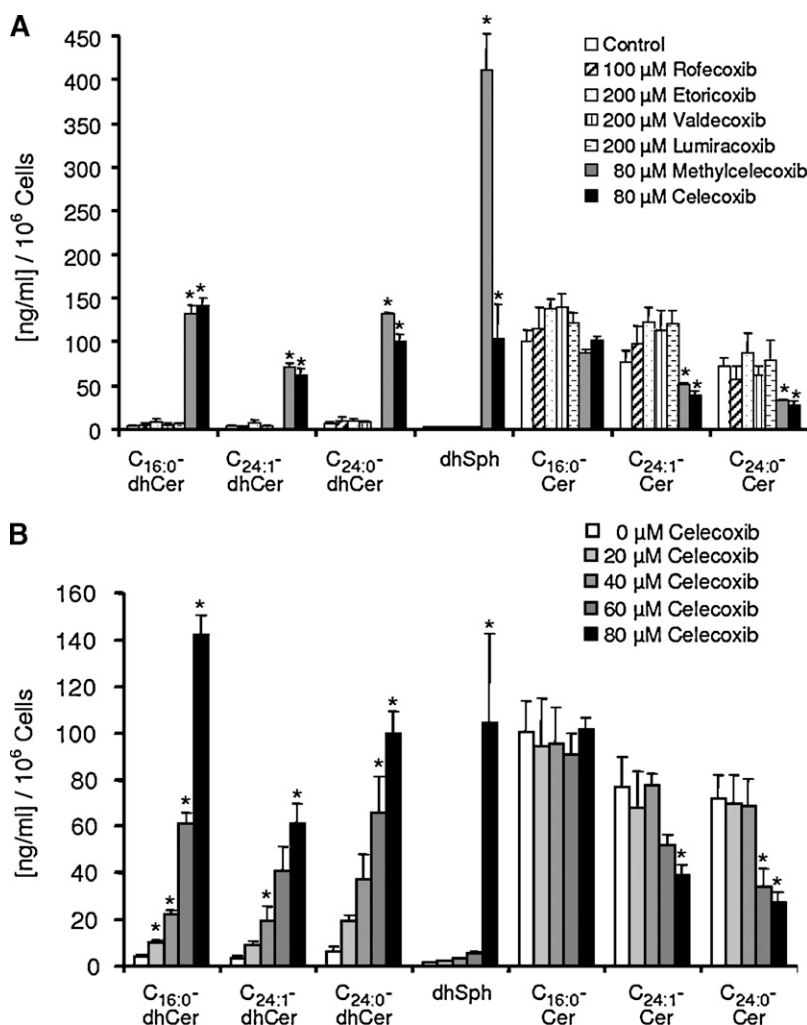


Fig. 2. The effects of coxibs on the sphingolipid level. HCT-116 cells were treated for 2 h either with various coxibs [rofecoxib (100 μ M), etoricoxib (200 μ M), valdecoxib (200 μ M), lumiracoxib (200 μ M), methylcelecoxib (80 μ M), celecoxib (80 μ M)] or DMSO as control (A) or with increasing concentrations of celecoxib as indicated (B). The sphingolipid amounts determined by liquid chromatography tandem mass spectrometry (LC-MS/MS) were related to the number of treated cells. Data are mean \pm SEM of one of three comparable independent experiments, each performed in duplicate. * $P < 0.05$, significant difference between coxib-treated and control cells. Cer, ceramide; dhCer, dihydroceramide.

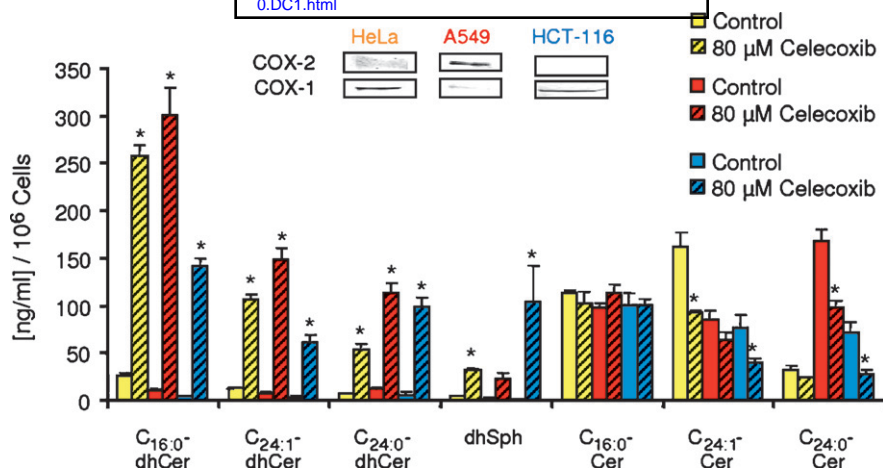


Fig. 3. Comparison of celecoxib-induced alterations of sphingolipid levels in various human cancer cells. Human cervix carcinoma cells HeLa (yellow), lung cancer cells A549 (red), and colon cancer cells HCT-116 (blue) were treated with either DMSO (control) or 80 μM celecoxib (striped bars) for 2 h. The sphingolipid amounts determined by LC-MS/MS were related to the number of treated cells. Data are mean \pm SEM of one of three comparable independent experiments, each performed in duplicate. * $P < 0.05$, significant difference between celecoxib-treated and control cells.

shows that in human colon cancer cells (HCT-116, COX-2 depleted/COX-1 expressing), in human cervix carcinoma cells (HeLa, COX-2 inducible/COX-1 expressing), and in human lung cancer cells (A549, COX-2 expressing/COX-1 expression very low), celecoxib treatment increased dhCer and dhSph levels and decreased $C_{24:1}$ - and $C_{24:0}$ -Cer levels. Other human colon cancer cells (HCA-7, HT-29), human breast cancer cells (MDA-MB231, MCF-7), and human embryonic kidney cells (HEK293) were tested and showed similar changes in the sphingolipid levels after celecoxib treatment (data not shown). These data clearly demonstrate that celecoxib-induced alterations in sphingolipid levels are a general COX-2-independent phenomenon that occurs in cell lines of various origins.

Celecoxib activates de novo sphingolipid synthesis and inhibits DEGS

Sphinganine and dhCers are nondurable intermediates of the sphingolipid pathway (Fig. 1). To investigate whether the increase of dhCer levels after celecoxib treatment originates from de novo sphingolipid biosynthesis or from the salvage pathway, an incorporation experiment with $^{13}\text{C}_3,^{15}\text{N}$ -labeled L-serine was performed. The addition of $^{13}\text{C}_3,^{15}\text{N}$ -labeled L-serine, a precursor of the sphingolipid de novo synthesis, leads to the production of labeled sphingolipids. This new labeling method enables us to discriminate by tandem mass spectrometry between sphingolipids generated by de novo synthesis and those generated by the salvage pathway. HCT-116 cells were treated with either 400 μM $^{13}\text{C}_3,^{15}\text{N}$ -labeled L-serine alone or with a combination of 400 μM $^{13}\text{C}_3,^{15}\text{N}$ -labeled L-serine and 80 μM celecoxib for times up to 6 h. In HCT-116 cells treated with $^{13}\text{C}_3,^{15}\text{N}$ -labeled L-serine, only labeled Cers were detected (Fig. 4; yellow/red bars). DhCers and dhSph were always low, probably owing to their immediate metabolism to Cer. In HCT-116 cells treated with $^{13}\text{C}_3,^{15}\text{N}$ -labeled L-serine and celecoxib, labeled dhCers and dhSph significantly in-

creased up to 6 h post treatment in a time-dependent manner, whereas the levels of $C_{24:1}$ - and $C_{24:0}$ -Cer significantly decreased (Fig. 4; white/blue bars). The strong accumulation of labeled dhCers and dhSph indicates that de novo sphingolipid biosynthesis is affected after celecoxib treatment and, additionally, that a significant decrease of $C_{24:0}$ - and $C_{24:1}$ -Cer is caused by an inhibition of the DEGS by celecoxib.

To confirm that celecoxib activates de novo sphingolipid biosynthesis, HCT-116 cells were treated with the L-SPT inhibitors myriocin (150 nM) or L-cycloserine (500 μM) (both concentrations do not compromise cell viability) and celecoxib (80 μM) for 2 h. Both inhibitors prevented the celecoxib-induced upregulation of dhCers (Supplement 3). Additionally, we compared the total amount of Cer (dhCer and Cer) in HCT-116 cells after treatment of cells with 80 μM celecoxib, 1 μM C8-CPPC (inhibitor of DEGS), 50 μM FB1 (inhibitor of CerS) and a DMSO control for 2 h (Fig. 5A). The inhibitors C8-CPPC and FB1 reduced Cer levels and increased dhCer or dhSph levels (data not shown) but mediated no alteration in the total Cer levels. In contrast, celecoxib significantly increased the total Cer level 2-fold. These data suggest that celecoxib activates de novo sphingolipid biosynthesis. However, in vitro (microsomal fractions of HCT-116 cells) activity assays of L-SPT and the dhCer synthase, the two pacemaker enzymes of the sphingolipid pathway, showed no increase in enzyme activity in the presence of celecoxib (Supplement 4), indicating that a cellular context is necessary for celecoxib-induced sphingolipid biosynthesis.

The concomitant increase of dhCers ($C_{16:0}$ -, $C_{24:1}$ -, and $C_{24:0}$ -dhCer) and decrease of Cers ($C_{24:1}$ - and $C_{24:0}$ -Cer) after celecoxib treatment suggest inhibition of the DEGS. To test this hypothesis, we performed an in vivo activity assay using the nonphysiological $C_{8:0}$ -dhCer as a substrate for the DEGS and measured the product $C_{8:0}$ -Cer by LC-MS/MS. HCT-116 cells were incubated for 2 h with

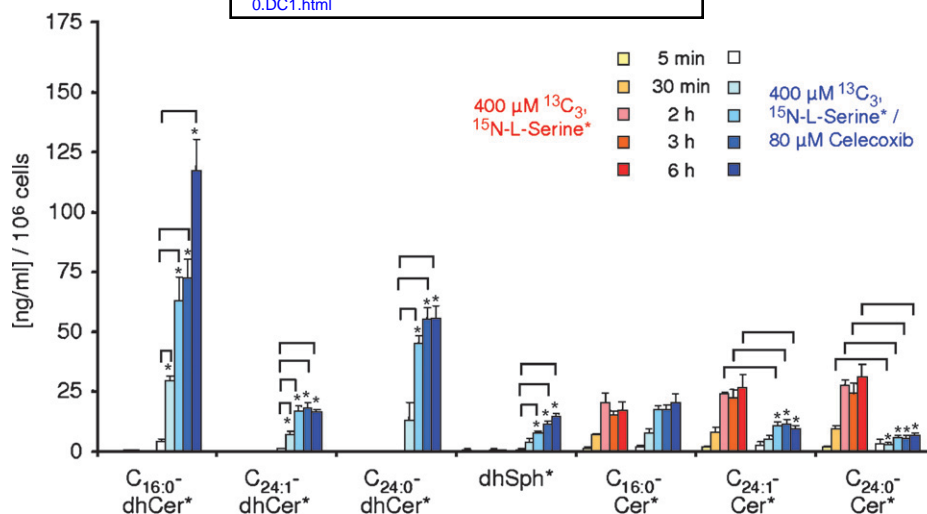


Fig. 4. A ^{13}C , ^{15}N -labeled L-serine incorporation experiment. HCT-116 cells were treated either with $400\ \mu\text{M}$ ^{13}C , ^{15}N -labeled L-serine (yellow/red bars) as control or cotreated with $400\ \mu\text{M}$ ^{13}C , ^{15}N -labeled L-serine and $80\ \mu\text{M}$ celecoxib (white/blue bars) up to 6 h. The labeled sphingolipids are marked with an asterisk. The labeled sphingolipid amounts determined by LC-MS/MS were related to the number of treated cells. Data are mean \pm SEM of three independent experiments, each performed in duplicate. * $P < 0.01$, significant difference in case of dhCers/sphinganine (dhSph) between celecoxib-treated cells at different time points and celecoxib-treated cells for 5 min and in case of Cers between celecoxib-treated and control cells at the indicated time points.

$10\ \mu\text{M}$ $\text{C}_{8:0}$ -dhCer and coincubated with increasing concentrations of celecoxib (0 – $120\ \mu\text{M}$) (Fig. 5B). The IC_{50} value for DEGS inhibition was $78.9 \pm 1.5\ \mu\text{M}$ with a maximum inhibition of 75% at $120\ \mu\text{M}$ (higher celecoxib concentrations induce cell death already after 2 h). This IC_{50} value fits with the observation that the levels of $\text{C}_{24:1}$ - and $\text{C}_{24:0}$ -Cer significantly decrease only at celecoxib concentrations $\geq 60\ \mu\text{M}$ (Fig. 2B).

The interaction of celecoxib with the acid or neutral SMase was also examined. These two enzymes were specifically inhibited with desipramine (inhibitor of the acid SMase) or glutathione (inhibitor of the neutral SMase) and coincubated the cells with celecoxib ($80\ \mu\text{M}$). Both inhibitors had no influence on celecoxib-induced sphingolipid alterations (data not shown).

The Cer biosynthesis inhibitors myriocin and L-cycloserine protect cells from celecoxib-induced anti-proliferative effects

To determine whether the elevated dhCer levels contributed to the apoptotic potency of celecoxib, cells were coincubated with myriocin, an inhibitor of the L-SPT. HCT-116 cells were either treated with $80\ \mu\text{M}$ celecoxib alone or cotreated with $150\ \text{nM}$ myriocin (a concentration that does not induce apoptosis) for 6 h, and the rate of apoptosis was determined using the APOPercentage assay. Cotreatment of cells with myriocin and celecoxib prevented upregulation of dhCers and dhSph after celecoxib treatment (Supplement 3) and reduced significantly celecoxib-induced apoptosis (Fig. 6A).

To address the question of whether the increased dhCer levels reduce cell viability, HCT-116 cells were treated with $80\ \mu\text{M}$ celecoxib alone or cotreated with either $150\ \text{nM}$ myriocin or with $500\ \mu\text{M}$ L-cycloserine (inhibitor of the

L-SPT) and assayed for cell viability using the WST-1 protocol. Cotreatment (20 h) of cells with increasing concentrations of celecoxib and myriocin (Fig. 6B) or L-cycloserine (Fig. 6C) (both substances inhibit the celecoxib-induced upregulation of dhCers; Supplement 3) had protective effects against the anti-proliferative effects of celecoxib. Therefore, we propose that an increase in dhCer or dhSph levels is partly responsible for celecoxib-induced cytotoxic effects. The reduced Cer levels do not seem to be of importance, inasmuch as myriocin alone reduced the Cer levels (Supplement 3) without inducing apoptosis or affecting cell viability.

DISCUSSION

Sphingolipids are important signaling molecules that regulate proliferation as well as apoptotic processes (28, 29). Because disruption of the balance between proliferating and anti-proliferating sphingolipids has dramatic consequences for the cell, and because certain coxibs mediate anti-proliferative effects through COX-2-independent pathways, we investigated the interaction of coxibs with the sphingolipid pathway. In this study, we showed that celecoxib and methylcelecoxib are the only coxibs that lead to an accumulation of dhCers in cancer cells through activation of de novo sphingolipid biosynthesis and inhibition of DEGS. All other coxibs tested had no effect on sphingolipid levels. The increase of dhCers after celecoxib treatment occurs already after 5 min, indicating modulation of nontranscriptional processes. Interestingly, accumulation of dhCers depends on the presence of celecoxib, because removing celecoxib from the cell culture medium returns the dhCer concentrations (data not shown) to

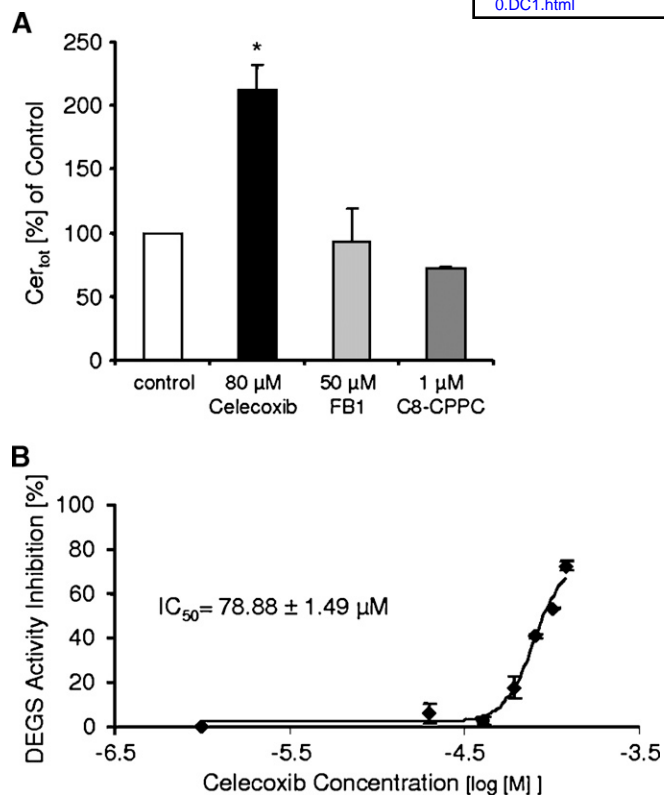


Fig. 5. A: The effect of celecoxib, C8-cyclopropenylceramide (C8-CPPC), and fumonisins B1 (FB1) on the total ceramide level. HCT-116 cells were treated with either DMSO (white bars), 80 μ M celecoxib (black bars), 50 μ M FB1 (light-gray bars), or 5 μ M C8-CPPC (gray bars) for 2 h. The sphingolipid amounts determined by LC-MS/MS were related to the sphingolipid amounts of DMSO-treated cells. Data are mean \pm SEM of three independent experiments, each performed in duplicate. * $P < 0.05$, significant difference between celecoxib- or C8-CPPC-treated cells versus untreated cells. B: In vivo DEGS activity in the presence of celecoxib. HCT-116 cells were cotreated with 10 μ M C_{8:0}-dhCer and increasing concentrations of celecoxib for 2 h. The amount of C_{8:0}-Cer was determined by LC-MS/MS. To calculate the IC₅₀ value for DEGS inhibition, the nonlinear regression analysis and a sigmoid E_{max} model were used. Experiments were done in triplicate; data are mean \pm SEM.

their basal levels. Furthermore, in vitro activity assays of the L-SPT and the dhCerS (Supplement 4) show no activation of either enzyme in the presence of celecoxib, indicating that a whole cell is necessary for celecoxib-induced de novo sphingolipid biosynthesis. Activation/inhibition of an enzyme may depend on post-translational modifications as well as cofactors and substrate availability. It is not clear which of these is responsible for the observed elevation of sphingolipid biosynthesis. Activation of SMase by accumulation of arachidonic acid due to inhibition of COX-2, as proposed by Chan et al. (30) for sulindac sulfide, cannot explain celecoxib-induced upregulation of dhCers because we show 1) that dhCers are produced via de novo synthesis and that SMases are not involved and 2) that other coxibs, which inhibit COX-2 even more potently than celecoxib, do not alter sphingolipid levels.

A decrease of C_{24:0}- and C_{24:1}-Cer levels after celecoxib treatment indicates that celecoxib inhibits DEGS. By per-

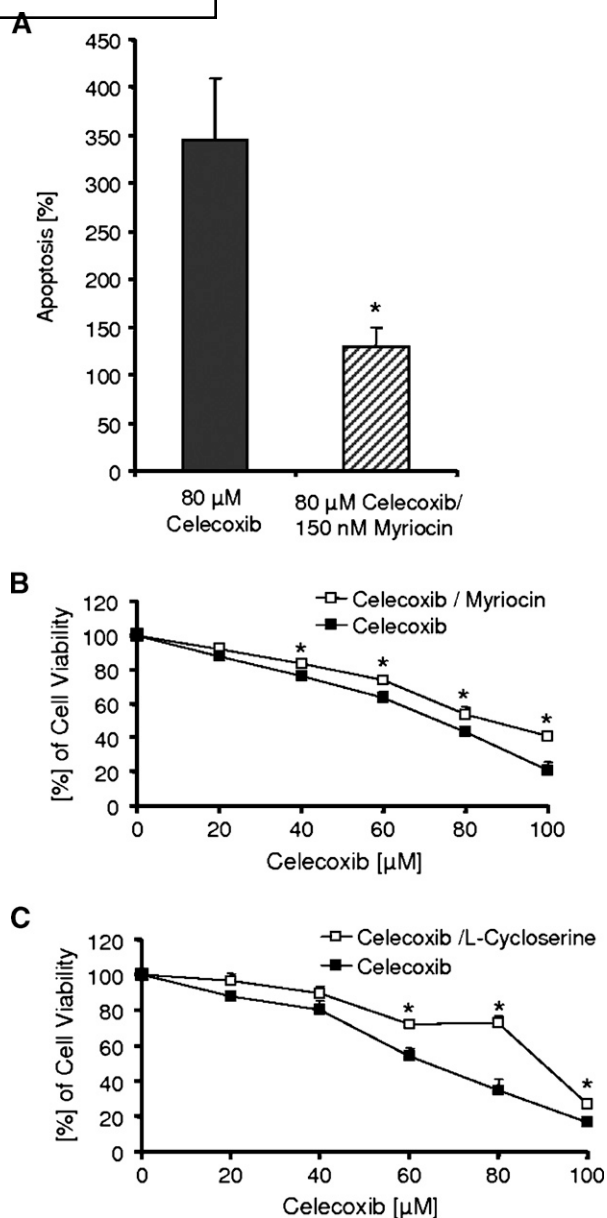



Fig. 6. Effect of myriocin and L-cycloserine on celecoxib-induced reduction of cell viability and apoptosis. A: HCT-116 cells were either incubated with 80 μ M celecoxib or cotreated with 80 μ M celecoxib and 150 nM myriocin for 6 h. The rate of apoptosis was analyzed using the APOPercentage kit as described. * $P < 0.01$, significant difference between celecoxib-treated cells versus celecoxib/myriocin-treated cells. B, C: HCT-116 cells were treated with increasing concentrations of celecoxib (black squares), as indicated, for 20 h or preincubated with either 150 nM myriocin (white squares) (B) or 500 μ M L-cycloserine (white squares) (C) for 90 min and then treated with increasing concentrations of celecoxib in the presence of 150 nM myriocin or 500 μ M L-cycloserine for 20 h. The cell viability was determined using WST-1 proliferation assay. The proliferation rate of untreated cells or cells treated only with myriocin or L-cycloserine was used as an index for 100% cell viability. The relative viability rate was then expressed as the ratio of the cell viability of treated versus untreated cells. Data are mean \pm SEM of three comparable independent experiments, each performed in triplicate. * $P < 0.05$, significant difference between celecoxib and celecoxib/myriocin- or celecoxib/L-cycloserine-treated cells.

forming an *in vivo* dhCer desaturase assay with non-physiological C_{8:0}-dhCer as substrate, we could demonstrate that celecoxib inhibits DEGS *in vivo* with an IC₅₀ of 78.9 ± 1.5 μM. Dihydroceramide desaturase 1 (DEGS1; with delta-4 desaturase activity) plays the predominant role in human cells, whereas DEGS2 (with an additional hydroxylase activity), which is less characterized, appears to play a minor role (31, 32). DEGS1 prefers short-chain dhCer substrates (33, 34). Incomplete inhibition of these enzymes, possibly by indirect mechanisms, could be mediated by changes in the membrane fluidity, owing to celecoxib (unpublished observations). Planar substances like celecoxib (35) and unsaturated lipids, like the upregulated dhCers, induce membrane rigidity. Membrane stiffening is proposed to affect the conformation and function of integral membrane proteins (36). DEGS is a protein complex consisting of a flavin-containing cytochrome b5 reductase, a heme-containing b5, and a non-heme-containing desaturase (33), whose quaternary structure would be sensitive to membrane consistency. Johnson et al. (37) observed an inhibition of the membrane protein Ca²⁺-ATPase by higher concentrations of celecoxib (IC₅₀ = 35 μM), which was connected to membrane effects of celecoxib by Gamerdinger, Clement, and Behl (35), indicating that celecoxib can influence enzyme activities by increasing membrane rigidity.

The use of the Cer biosynthesis inhibitors myriocin and L-cycloserine suggests that changes in dhCer levels contribute to the apoptosis-inducing and anti-proliferative activity of celecoxib. Moreover, the specific inhibitor C8-CPPC (5 μM) reduced the cell viability of HCT-116 cells to 15% (Supplement 5). In the presence of myriocin, the reduction is attenuated to only 28%. In contrast, exogenously added dhCers induce no apoptosis or cell cycle arrest. A recent report demonstrated that the location of the synthesized Cer is essential for the mode of action (3). Additionally, *in vivo* studies support the notion that endogenously produced dhCers act like Cers. Munoz-Olaya et al. (38) showed that Jurkat A3 cells treated with XM462 (inhibitor of DEGS) exhibit increased dhCer levels and reduced cell viability. Additionally, Jiang et al. (39) could also demonstrate for the chemotherapeutic γ-tocopherole, which blocks the DEGS, that an accumulation of endogenously produced C_{16:0}-dhCer induces apoptosis in lung cancer cells (A549). Moreover, Tserng and Griffin (40) elucidated that natural C_{16:0}-Cer exogenously added to human leukemia cells induces apoptosis via accumulation of dhCers. Deregulation of dhCer and Cer levels in fibroblasts, caused by the loss of the CLN9 gene, has dramatic consequences for cell growth, inasmuch as these cells show rapid growth on the one hand but increased apoptosis on the other hand (41). Kravka et al. (32) demonstrated that fenretinide increases the concentration of dhCer through inhibition of DEGS, which was associated with an upregulated dhCer level, activation of protein phosphatase PP1, and a subsequent dephosphorylation of retinoblastoma protein (RB), a set of events that resulted in cell cycle arrest. Furthermore, fenretinide induces in human prostate cancer cells also an increase of C_{16:0}-dhCer, C_{24:1}-dhCer, and C_{24:0}-dhCer and a slight decrease of C_{24:1}-Cer and C_{24:0}-Cer. The authors

linked this increase of dhCers to the induction of autophagy (42). Together, the body of evidence strongly indicates that dhCers could be relevant mediators of cytotoxic effects. In addition to raised dhCer levels, it is also possible that the changes in Cer levels contribute to the induction of apoptosis after celecoxib treatment. Liu et al. (43) recently proposed that the balance between C_{16:0}- and C_{24:0}-Cer plays an important role in inducing apoptosis. Interestingly, the pro-apoptotic C_{16:0}-Cer remains unchanged after celecoxib treatment, whereas the anti-apoptotic C_{24:0}-Cer decreases; the balance is therefore tipped toward apoptosis. In the case of celecoxib, the modulation of sphingolipid levels appears to be a unique response, because it was observed in various cancer cell lines, and it seems to be COX-2 independent, because it occurs in COX-2-overexpressing and COX-2-depleted cell lines (Fig. 3). This tenet was further confirmed by the fact that other selective COX-2 inhibitors show no effect on sphingolipid levels (Fig. 2A).

In conclusion, we demonstrated for the first time that treatment of cells with celecoxib activates *de novo* sphingolipid synthesis and inhibits DEGS, which leads to a rapid cellular accumulation of C_{16:0}-, C_{24:0}-, and C_{24:1}-dhCers and depletion of long-chain C_{24:0}- and C_{24:1}-Cers. Furthermore, the increase of dhCer levels appears to be relevant for the cytotoxic effect of celecoxib. 

REFERENCES

1. Pettus, B. J., C. E. Chalfant, and Y. A. Hannun. 2002. Ceramide in apoptosis: an overview and current perspectives. *Biochim. Biophys. Acta.* **1585**: 114–125.
2. Ruvolo, P. P. 2003. Intracellular signal transduction pathways activated by ceramide and its metabolites. *Pharmacol. Res.* **47**: 383–392.
3. Hannun, Y. A., and L. M. Obeid. 2008. Principles of bioactive lipid signalling: lessons from sphingolipids. *Nat. Rev. Mol. Cell Biol.* **9**: 139–150.
4. Pewzner-Jung, Y., S. Ben-Dor, and A. H. Futerman. 2006. When do Lassus (longevity assurance genes) become CerS (ceramide synthases)? Insights into the regulation of ceramide synthesis. *J. Biol. Chem.* **281**: 25001–25005.
5. Schmelz, E. M., P. C. Roberts, E. M. Kustin, L. A. Lemonnier, M. C. Sullards, D. L. Dillehay, and A. H. Merrill, Jr. 2001. Modulation of intracellular beta-catenin localization and intestinal tumorigenesis *in vivo* and *in vitro* by sphingolipids. *Cancer Res.* **61**: 6723–6729.
6. Ahn, E. H., and J. J. Schroeder. 2006. Sphinganine causes early activation of JNK and p38 MAPK and inhibition of AKT activation in HT-29 human colon cancer cells. *Anticancer Res.* **26**: 121–127.
7. Huwiler, A., and J. Pfeilschifter. 2006. Altering the sphingosine-1-phosphate/ceramide balance: a promising approach for tumor therapy. *Curr. Pharm. Des.* **12**: 4625–4635.
8. Cuvillier, O. 2007. Sphingosine kinase-1—a potential therapeutic target in cancer. *Anticancer Drugs.* **18**: 105–110.
9. Grosch, S., I. Tegeder, E. Niederberger, L. Brautigam, and G. Geisslinger. 2001. COX-2 independent induction of cell cycle arrest and apoptosis in colon cancer cells by the selective COX-2 inhibitor celecoxib. *FASEB J.* **15**: 2742–2744.
10. Kim, S. H., S. H. Song, S. G. Kim, K. S. Chun, S. Y. Lim, H. K. Na, J. W. Kim, Y. J. Surh, Y. J. Bang, and Y. S. Song. 2004. Celecoxib induces apoptosis in cervical cancer cells independent of cyclooxygenase using NF-kappaB as a possible target. *J. Cancer Res. Clin. Oncol.* **130**: 551–560.
11. Liu, X., P. Yue, Z. Zhou, F. R. Khuri, and S. Y. Sun. 2004. Death receptor regulation and celecoxib-induced apoptosis in human lung cancer cells. *J. Natl. Cancer Inst.* **96**: 1769–1780.

12. Basu, G. D., L. B. Pathangey, T. L. Tinder, S. J. Gendler, and P. Mukherjee. 2005. Mechanisms underlying the growth inhibitory effects of the cyclo-oxygenase-2 inhibitor celecoxib in human breast cancer cells. *Breast Cancer Res.* **7**: R422–R435.
13. Grosch, S., T. J. Maier, S. Schiffmann, and G. Geisslinger. 2006. Cyclooxygenase-2 (COX-2)-independent anticarcinogenic effects of selective COX-2 inhibitors. *J. Natl. Cancer Inst.* **98**: 736–747.
14. Arber, N., C. J. Eagle, J. Spicak, I. Racz, P. Dite, J. Hajer, M. Zavoral, M. J. Lechuga, P. Gerletti, J. Tang, et al. 2006. Celecoxib for the prevention of colorectal adenomatous polyps. *N. Engl. J. Med.* **355**: 885–895.
15. Bertagnolli, M. M., C. J. Eagle, A. G. Zauber, M. Redston, S. D. Solomon, K. Kim, J. Tang, R. B. Rosenstein, J. Wittes, D. Corle, et al. 2006. Celecoxib for the prevention of sporadic colorectal adenomas. *N. Engl. J. Med.* **355**: 873–884.
16. Baron, J. A., R. S. Sandler, R. S. Bresalier, H. Quan, R. Riddell, A. Lanasa, J. A. Bolognese, B. Oxenius, K. Horgan, S. Loftus, et al. 2006. A randomized trial of rofecoxib for the chemoprevention of colorectal adenomas. *Gastroenterology.* **131**: 1674–1682.
17. Bresalier, R. S., R. S. Sandler, H. Quan, J. A. Bolognese, B. Oxenius, K. Horgan, C. Lines, R. Riddell, D. Morton, A. Lanasa, et al. 2005. Cardiovascular events associated with rofecoxib in a colorectal adenoma chemoprevention trial. *N. Engl. J. Med.* **352**: 1092–1102.
18. Maier, T. J., A. Janssen, R. Schmidt, G. Geisslinger, and S. Grosch. 2005. Targeting the beta-catenin/APC pathway: a novel mechanism to explain the cyclooxygenase-2-independent anticarcinogenic effects of celecoxib in human colon carcinoma cells. *FASEB J.* **19**: 1353–1355.
19. Fillet, M., M. Bentires-Alj, V. Derégowski, R. Greimers, J. Gielen, J. Piette, V. Bours, and M. P. Merville. 2003. Mechanisms involved in exogenous C2- and C6-ceramide-induced cancer cell toxicity. *Biochem. Pharmacol.* **65**: 1633–1642.
20. Zhu, J., J. W. Huang, P. H. Tseng, Y. T. Yang, J. Fowble, C. W. Shiau, Y. J. Shaw, S. K. Kulp, and C. S. Chen. 2004. From the cyclooxygenase-2 inhibitor celecoxib to a novel class of 3-phosphoinositide-dependent protein kinase-1 inhibitors. *Cancer Res.* **64**: 4309–4318.
21. Kulp, S. K., Y. T. Yang, C. C. Hung, K. F. Chen, J. P. Lai, P. H. Tseng, J. W. Fowble, P. J. Ward, and C. S. Chen. 2004. 3-Phosphoinositide-dependent protein kinase-1/Akt signaling represents a major cyclooxygenase-2-independent target for celecoxib in prostate cancer cells. *Cancer Res.* **64**: 1444–1451.
22. Perry, D. K., J. Carton, A. K. Shah, F. Meredith, D. J. Uhlinger, and Y. A. Hannun. 2000. Serine palmitoyltransferase regulates de novo ceramide generation during etoposide-induced apoptosis. *J. Biol. Chem.* **275**: 9078–9084.
23. Lin, C. F., C. L. Chen, W. T. Chang, M. S. Jan, L. J. Hsu, R. H. Wu, M. J. Tang, W. C. Chang, and Y. S. Lin. 2004. Sequential caspase-2 and caspase-8 activation upstream of mitochondria during ceramide and etoposide-induced apoptosis. *J. Biol. Chem.* **279**: 40755–40761.
24. Charles, A. G., T. Y. Han, Y. Y. Liu, N. Hansen, A. E. Giuliano, and M. C. Cabot. 2001. Taxol-induced ceramide generation and apoptosis in human breast cancer cells. *Cancer Chemother. Pharmacol.* **47**: 444–450.
25. Wang, H., B. J. Maurer, C. P. Reynolds, and M. C. Cabot. 2001. N-(4-hydroxyphenyl)retinamide elevates ceramide in neuroblastoma cell lines by coordinate activation of serine palmitoyltransferase and ceramide synthase. *Cancer Res.* **61**: 5102–5105.
26. Brautigam, L., G. Vetter, I. Tegeder, G. Heinkele, and G. Geisslinger. 2001. Determination of celecoxib in human plasma and rat microdialysis samples by liquid chromatography tandem mass spectrometry. *J. Chromatogr. B Biomed. Sci. Appl.* **761**: 203–212.
27. Schmidt, H., R. Schmidt, and G. Geisslinger. 2006. LC-MS/MS-analysis of sphingosine-1-phosphate and related compounds in plasma samples. *Prostaglandins Other Lipid Mediat.* **81**: 162–170.
28. Hannun, Y. A. 1996. Functions of ceramide in coordinating cellular responses to stress. *Science.* **274**: 1855–1859.
29. Spiegel, S., and A. H. Merrill, Jr. 1996. Sphingolipid metabolism and cell growth regulation. *FASEB J.* **10**: 1388–1397.
30. Chan, T. A., P. J. Morin, B. Vogelstein, and K. W. Kinzler. 1998. Mechanisms underlying nosteroidal antiinflammatory drug-mediated apoptosis. *Proc. Natl. Acad. Sci. USA.* **95**: 681–686.
31. Ternes, P., S. Franke, U. Zahringer, P. Sperling, and E. Heinz. 2002. Identification and characterization of a sphingolipid delta 4-desaturase family. *J. Biol. Chem.* **277**: 25512–25518.
32. Kravka, J. M., L. Li, Z. M. Szulc, J. Bielawski, B. Ogretmen, Y. A. Hannun, L. M. Obeid, and A. Bielawska. 2007. Involvement of dihydroceramide desaturase in cell cycle progression in human neuroblastoma cells. *J. Biol. Chem.* **282**: 16718–16728.
33. Michel, C., G. van Echten-Deckert, J. Rother, K. Sandhoff, E. Wang, and A. H. Merrill, Jr. 1997. Characterization of ceramide synthesis. A dihydroceramide desaturase introduces the 4,5-trans-double bond of sphingosine at the level of dihydroceramide. *J. Biol. Chem.* **272**: 22432–22437.
34. Mikami, T., M. Kashiwagi, K. Tsuchihashi, T. Akino, and S. Gasa. 1998. Substrate specificity and some other enzymatic properties of dihydroceramide desaturase (ceramide synthase) in fetal rat skin. *J. Biochem. (Tokyo).* **123**: 906–911.
35. Gamberdinger, M., A. B. Clement, and C. Behl. 2007. Cholesterol-like effects of selective cyclooxygenase inhibitors and fibrates on cellular membranes and amyloid-beta production. *Mol. Pharmacol.* **72**: 141–151.
36. Maxfield, F. R., and I. Tabas. 2005. Role of cholesterol and lipid organization in disease. *Nature.* **438**: 612–621.
37. Johnson, A. J., A. L. Hsu, H. P. Lin, X. Song, and C. S. Chen. 2002. The cyclo-oxygenase-2 inhibitor celecoxib perturbs intracellular calcium by inhibiting endoplasmic reticulum Ca²⁺-ATPases: a plausible link with its anti-tumour effect and cardiovascular risks. *Biochem. J.* **366**: 831–837.
38. Munoz-Olaya, J. M., X. Matabosch, C. Bedia, M. Egidio-Gabas, J. Casas, A. Llebaria, A. Delgado, and G. Fabrias. 2008. Synthesis and biological activity of a novel inhibitor of dihydroceramide desaturase. *ChemMedChem.* **3**: 946–953.
39. Jiang, Q., J. Wong, H. Fyrrst, J. D. Saba, and B. N. Ames. 2004. Gamma-tocopherol or combinations of vitamin E forms induce cell death in human prostate cancer cells by interrupting sphingolipid synthesis. *Proc. Natl. Acad. Sci. USA.* **101**: 17825–17830.
40. Tserng, K. Y., and R. L. Griffin. 2004. Ceramide metabolite, not intact ceramide molecule, may be responsible for cellular toxicity. *Biochem. J.* **380**: 715–722.
41. Schulz, A., T. Mousallem, M. Venkataramani, D. A. Persaud-Sawin, A. Zucker, C. Luberto, A. Bielawska, J. Bielawski, J. C. Holthuis, S. M. Jazwinski, et al. 2006. The CLN9 protein, a regulator of dihydroceramide synthase. *J. Biol. Chem.* **281**: 2784–2794.
42. Zheng, W., J. Kollmeyer, H. Symolon, A. Momin, E. Munter, E. Wang, S. Kelly, J. C. Allegood, Y. Liu, Q. Peng, et al. 2006. Ceramides and other bioactive sphingolipid backbones in health and disease: lipidomic analysis, metabolism and roles in membrane structure, dynamics, signaling and autophagy. *Biochim. Biophys. Acta.* **1758**: 1864–1884.
43. Liu, X., S. Elojeimy, L. S. Turner, A. E. Mahdy, Y. H. Zeidan, A. Bielawska, J. Bielawski, J. Y. Dong, A. M. El-Zawahry, G. W. Guo, et al. 2008. Acid ceramidase inhibition: a novel target for cancer therapy. *Front. Biosci.* **13**: 2293–2298.